



The temporal variation of radon concentration at different depths of soil: A case study in Beijing

Yucai Mao^a, Lei Zhang^{b,*}, Hao Wang^{a,b}, Qiuju Guo^a

^a State Key Laboratory of Nuclear Physics and Technology, School of Physics, Peking University, Beijing, 100871, China

^b State Key Laboratory of NBC Protection for Civilian, Beijing, 102205, China

ARTICLE INFO

Keywords:

Radon concentration in soil
Temporal variation
Continuous measurement
Fast Fourier transform
Residual analysis

ABSTRACT

Variations in soil radon concentrations are a potential precursor of earthquake and volcanic events. However, the unclear migration and variation mechanisms of radon concentrations in soil still limit its effective application. To elucidate the temporal variation and its possible influence factors on radon concentrations at different soil depths, a case study was performed at a suburban site in Beijing. A long-term continuous measurement system consisting of ten radon-in-soil monitors at depths from 0.1 to 5.0 m and other meteorological sensors was employed. The monitoring was carried out from January 8th to July 29th, 2022, covering 3445 h in total. Radon concentrations generally increased with soil depth. Diurnal variation of soil radon concentrations at depths of 1.2 and 1.6 m in winter and spring was observed, and a negative correlation between the soil radon concentration and the residual air pressure was found. This finding indicates a possible air exchange channel between the soil and the atmosphere at the study site. In addition, the soil radon concentration at 4.0 m depth was unexpectedly lower than that of neighboring depths and was steady throughout the measurement period. This is attributed to a possible clay layer in the soil structure at 4.0 m depth. The results of this field study indicate that the complexity of temporal variation of soil radon concentrations should be considered for its application in predicting earthquake and volcanic events.

1. Introduction

Radon (^{222}Rn) is a naturally occurring monoatomic radioactive noble gas, which is generated from the alpha decay of radium (^{226}Ra) in the uranium (^{238}U) decay chain. Since ^{226}Ra and ^{238}U are ubiquitous in natural environments such as soil, rocks and waterbodies, radon is widely distributed in the natural world. Because of its unique physical and chemical characteristics, radon has been adopted as a potential precursor gas for earthquake and volcanic event forecasts (Hwa et al., 2015; Cigolini et al., 2005). Historically, anomalous radon concentrations in soil have been observed several times preceding large earthquakes (Vaupotic et al., 2010; Ren et al., 2012; Das et al., 2009). However, there are still gaps in understanding the use of radon in soil as an effective precursor for predicting earthquakes and volcanic eruptions worldwide. One of the main reasons is the difficulty in discriminating between anomalies caused by physical processes occurring in the Earth's upper crust and natural variation caused by local meteorological parameters.

Radon concentration in soil is influenced by many meteorological

parameters, including soil temperature, soil humidity, atmospheric pressure, air temperature and rainfall amongst others (Wang et al., 2021; Catalano et al., 2015; Pinault and Baubron, 1996). Hence, for the purpose of earthquake forecast, the ideal monitoring of radon in soil should not only be sensitive to the anomalous change caused by geological activity but should also avoid or minimize meteorological-induced variations. To reach this goal, a suitable depth to install a radon detector in soil is a key point, especially for online seismic observation. In practice, monitoring of radon concentration in soil is mainly conducted at depths from 0.5 to 1.0 m (Kemski et al., 2001; Buttafuoco et al., 2010; Han et al., 2014; Chen et al., 2018; Dhar et al., 2021). Buttafuoco et al. suggested that such a depth (0.5–1.0 m) could avoid the influence of meteorological factors on radon concentration in soil (Buttafuoco et al., 2010). However, several field studies indicate that radon concentration can still fluctuate due to the influence of meteorological factors at this soil depth (Catalano et al., 2015; Zafir et al., 2016; Haquin et al., 2022; Nazaroff, 1992). Friedmann even reported a contrary conclusion that the most sensitive depth to detect changes caused by meteorological factors is 0.5–1.0 m (Friedmann,

* Corresponding author.

E-mail address: swofely@pku.edu.cn (L. Zhang).

<https://doi.org/10.1016/j.jenvrad.2023.107200>

Received 10 January 2023; Received in revised form 25 April 2023; Accepted 2 May 2023

Available online 19 May 2023

0265-931X/© 2023 Elsevier Ltd. All rights reserved.

2012). Hence, deeper observations of radon concentrations in soil were carried out in China from 2.0 to 5.0 m at different seismic stations (Chen et al., 2019).

There are also different conclusions on the vertical distribution of radon concentration in soil with depth and its variation pattern. Results of some field measurements suggest that radon concentration in soil can exhibit a saturation phenomenon at a depth of about 0.8–1.3 m (Catalano et al., 2015; Barnet and Pacherová, 2016; Mitev et al., 2018). However, Antonopoulos-Domis et al. measured radon concentration at a depth of 0–2.6 m and reported that it increased with depth, remained constant between 0.8 and 1.3 m depth and then increased again, which indicated the existence of a two-layer soil structure with different diffusion-advection characteristics (Antonopoulos-Domis et al., 2009). The complexity caused by local characteristics of soil structure differing among regions and observation sites brings a great challenge for the practical application of radon concentration in soil as a precursor for predicting earthquake and volcanic events.

This study aims to elucidate the mechanisms of the distribution and variation of radon concentration in soil. Specifically, to figure out the temporal variation of radon concentration in soil up to a depth of 5.0 m, its variation pattern, and possible influence factors. Thus, field measurement was carried out with a long-term continuous monitoring system at a selected suburban site near Beijing for a case study.

2. Materials and methods

2.1. Design of field measurements

Field measurements were carried out at an abandoned farmland site (40.21656° N, 116.48722° E) in the suburban area of Beijing (Fig. 1). This farmland is free of human activity and remains a near-natural environment. Its soil characteristics and radon exhalation rate were studied many years ago (Sun et al., 2004). The site is about 4.2 km northwest of the Huangzhuang-Gaoliying fault, which is a field observation site for seismic activity.

To study the temporal variation of radon concentration in soil at different depths and to achieve continuous and simultaneous measurements, NRSM-D01 radon-in-soil monitors (Sairatec Inc., China) were installed at ten depths varying from 0.1 to 5.0 m. In addition, to study the influence of meteorological parameters on radon concentration in soil, different sensors were also used to record soil temperatures, air temperature-humidity, air pressure and rain status. All monitors and sensors were connected and controlled by a control unit, and all data were automatically recorded at a 1-h cycle. A schematic diagram of the measurement system is shown in Fig. 2.

As shown in Fig. 2, radon monitors at 0.1 and 0.3 m were buried in

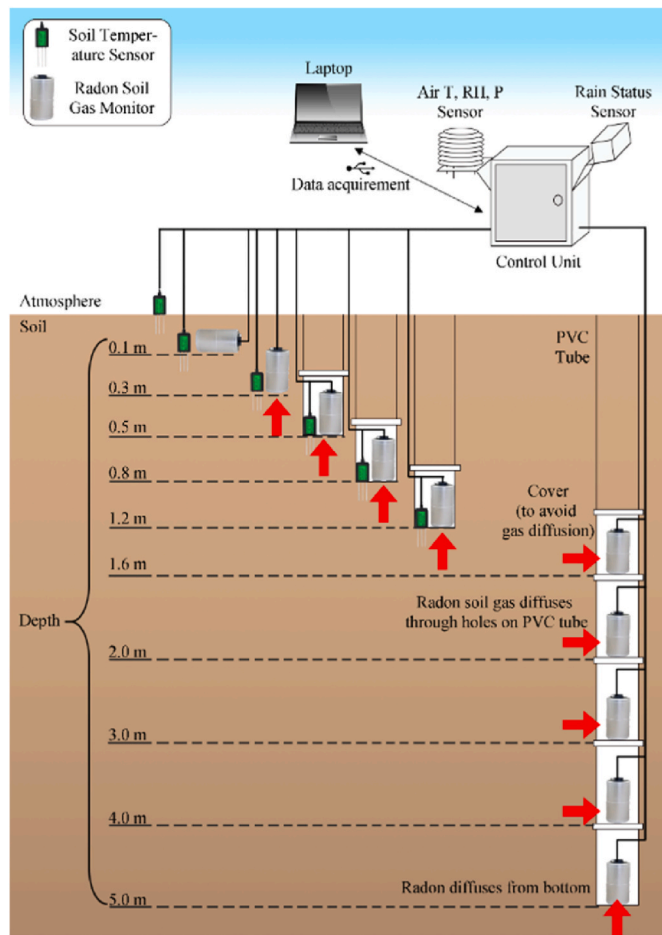


Fig. 2. Schematic diagram of the measurement system.

soil directly. Monitors at depths of 0.5–1.2 m were installed separately in 75 mm diameter PVC tubes with lids and covered by soil to prevent radon gas entering from above and to make radon gas only diffuse into the monitors from below. Monitors at depths from 1.6 to 5.0 m were installed inside a 5.0 m length tube, with some 2 mm diameter holes made on the tube wall to make radon gas diffuse freely. Six soil temperature sensors (MS10, Dalian Endeavour Technology Co., China) were installed on the soil surface and beside radon monitors at depths from 0.1 to 1.2 m. A temperature-humidity sensor (SHT31, Sensirion AG,

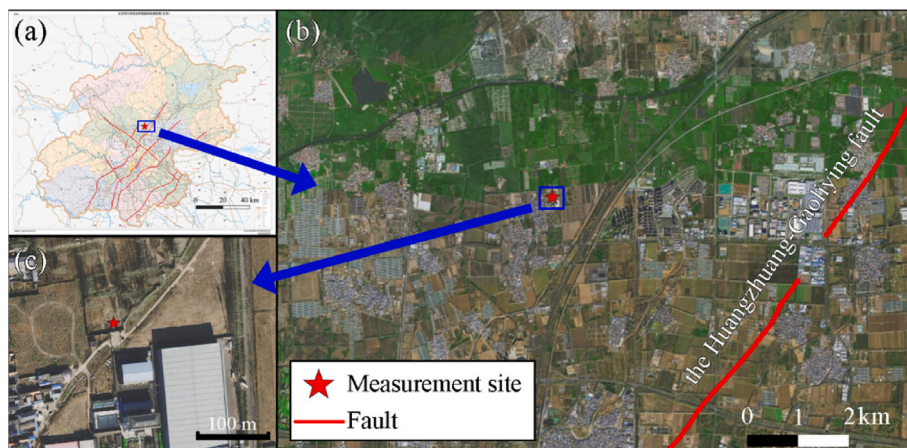


Fig. 1. (a) Map of faults in the Beijing area. (b) Location of measurement site and the Huangzhuang-Gaoliying fault. (c) High resolution satellite imagery of measurement site.

Switzerland) and a pressure sensor (BME280, Bosch Sensortec GmbH, Germany) were installed inside the instrument shelter. A rain status sensor (GD-YX016, Zhengzhou GONDY Technology Co., China) was employed to record the rainfall time.

Radon concentration in soil and meteorological parameters were monitored for two periods: 1) from January 8th to April 27th, 2022; and 2) from June 24th to July 29th, 2022. The first period covered 2619 h, and the second covered 826 h. These two periods covered the typical seasons of winter, spring, and summer in Beijing.

2.2. Measurement of radon-in-soil concentration, soil ²²⁶Ra and water content

The radon monitor used in this study was developed specifically for continuous measurement of radon concentration in soil, and is based on electrostatic collection and alpha spectrometry analysis techniques. Radon in soil gas diffuses into a 46.4 ml measurement chamber by passing through a waterproofing membrane and then a PTFE filter. The sensitivity of the NRS-M-D01 monitor is nearly 0.02 counts per hour/(Bq·m⁻³) at an absolute humidity of 18.5 g m⁻³ (25 °C, 80% RH). The minimum detection limit is about 230 ± 15 Bq·m⁻³ for the 1-h cycle. The uncertainty is less than 9% for a typical soil radon concentration of 15000 Bq·m⁻³ (Wang et al., 2021).

Soil samples were collected using a Luoyang shovel at different depths while digging the 5.0 m hole on December 1st, 2021. The Luoyang shovel is a traditional tool for geological exploration that causes minimal damage to soil structure. Its single sampling length is nearly 0.3 m. Because the radium concentration basically does not change with time and the main focus is the layer structure of soil in different depths, a series of nine samples in different depths was collected. Due to the difference between the single sampling length of the Luoyang shovel and the length of radon-in-soil monitor with PVC tube, the depths of soil samples and the monitoring depths differed slightly.

The water contents and the ²²⁶Ra concentrations of soil samples were measured according to the method specified in ISO 11465:1993 (Soil quality, 1993) and ISO 18589-3:2015 (Measurement of radioactivity in the, 2015), respectively. The water contents of soil samples (η) were calculated by:

$$\eta = \frac{W_1 - W_2}{W_1 - W_3} \times 100\%$$

Here, W_1 stands for the total weight of soil sample with tray before drying (g); W_2 stands for the total weight of soil sample with tray after drying (g); W_3 stands for the weight of tray after cleaning (g).

The γ -energy spectra were measured by an anti-Compton HPGe detector (GMX60, Ortec, U.S.) with a relative efficiency of 60.4% and minimum detection limit of 0.12 Bq for ²²⁶Ra. A standard reference soil sample was used in calibration and quality assurance process. The ²²⁶Ra content of reference sample was calibrated in the National Institute of Metrology of China on August 21st, 2019. The energy peak counts of ²¹⁴Bi at 609.31 keV were measured, and the ²²⁶Ra concentrations (C_{Ra}) of the soil samples were calculated by:

$$C_{Ra} = \frac{A_{Ra}}{W} = \frac{A_{214Bi}}{W} = \frac{A_{Ra}^S}{W} \cdot \left(\frac{N_{Bi}^i}{t^i} - \frac{N_{Bi}^{BG}}{t^{BG}} \right) \cdot \frac{t^S}{N_{Bi}^S}$$

W is the net weight of soil sample (g); A_{Ra} is the radioactivity of ²²⁶Ra (Bq), which is equal to that of ²¹⁴Bi (A_{214Bi}) at radioactive equilibrium after one-month sealed; N_{Bi} is the gamma counts of ²¹⁴Bi at 609.31 keV; t is the measurement time of the HPGe detector (s). The superscripts of i , BG, S stand for the corresponding values of soil samples, background and the standard sample, respectively.

For the quality control of measurement, radon monitors were not only calibrated before the long-term monitoring, but also sent to a radon chamber again for verification after the field measurement. Those

calibrations and comparisons were carried out by taking an Alpha-GUARD PQ2000 (Saphymo, France) as a reference device, which could be traced to the National Institute of Metrology, China.

3. Results and discussion

3.1. Water content and ²²⁶Ra concentration of soil samples

The results of water contents and ²²⁶Ra concentrations of soil samples are presented in Table 1.

The water contents vary from 19.7 to 45.0%. The highest value appears at 0.1 m, which is attributed to the snowfall one day before the sample collection. The second highest value is at 1.8 m, and the lowest value is at 4.0 m. There is no difference over two standard deviations in water content at the rest of the depths. The ²²⁶Ra concentrations vary from 30.0 to 41.8 Bq·kg⁻¹. The soil sample at 4.0 m depth exhibited the lowest ²²⁶Ra concentration. As for soil classification, the soil of this site is sandy loam soil in general (Sun et al., 2004). However, by comparing the distributions of water content and Ra concentration, a special layer seems to be found at 4.0 m, which was different from other depths. Considering its yellow color and viscous texture, it is presumed to be a clay layer.

3.2. Radon concentration and meteorological data

The measurement results of radon and meteorological parameters are shown in Fig. 3 for both the January to April (Fig. 3(a)) and June to July (Fig. 3(b)) measurement periods. In general, soil radon concentration increased with depth, except for the unexpectedly low value at 4.0 m. Diurnal variations of soil radon concentration at depths from 0.8 to 3.0 m were clear. In addition, for meteorological parameters, soil temperature increased gradually from winter to summer and its diurnal variation in near surface layers was clear. Gradual increase of both air temperature and humidity was also noticeable (Fig. 3).

Soil radon concentrations in shallow layers (0.1–0.5 m) were relatively stable in winter and spring (Fig. 3(a)), while they varied irregularly and violently in summer (Fig. 3(b)). This was caused by the frequent rainfall in summer as indicated by the rain status shown in Fig. 3(b), which leads to an increase of soil humidity. A previous study found that the radon concentration rises rapidly in the near surface after rain (Wang et al., 2021). Radon concentration in the middle layer (0.8–3.0 m) fluctuated violently in winter and spring (Fig. 3(a)), but this phenomenon was not found in summer (Fig. 3(b)). The soil radon concentration at 5.0 m increased by approximately 100% in summer compared with that in winter and spring, and a gradual upward trend of radon concentration was observed from April 9th. The increase of soil radon concentration at 5.0 m does not originate from the influence of rainfall because there is no such tendency in radon concentration in the shallower soil layers. It is presumed to be caused by the change in groundwater level which usually varies from 4.0 to 7.0 m in this area (Yang et al., 2021).

Table 1
Water content and ²²⁶Ra concentration at different soil depths.

Depth (m)	Water Content	²²⁶ Ra Concentration (Bq·kg ⁻¹)
0.1	45.0%	35.3 ± 2.6
0.4	20.3%	39.8 ± 3.0
0.7	21.8%	35.1 ± 2.7
1.2	24.2%	33.9 ± 2.6
1.8	30.4%	41.8 ± 3.1
2.5	24.7%	34.0 ± 2.4
3.0	24.4%	34.6 ± 2.4
4.0	19.7%	30.0 ± 2.8
5.0	26.3%	37.6 ± 2.9

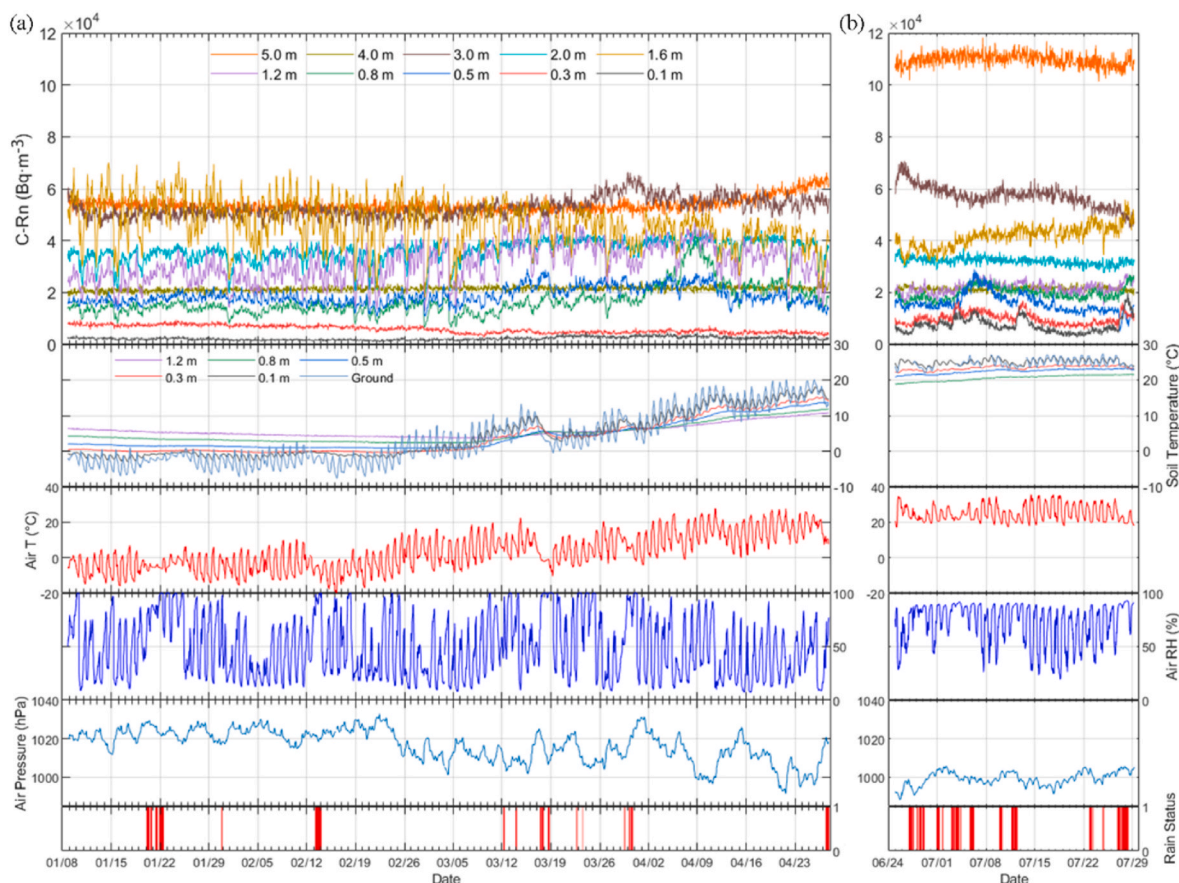


Fig. 3. Measurement results: (a) (left) data from January 8th to April 27th; and (b) (right) data from June 24th to July 29th (from the top to bottom, the plots show radon concentration in soil, soil temperature, air temperature, air relative humidity, air pressure and rain status).

3.3. Vertical distribution of radon concentration in soil

To observe the vertical distribution of soil radon concentration in different seasons at the study site and exclude the interference of meteorological parameters as far as possible, one typical sunny day with stable climate conditions was selected for each season. The criteria for selecting the typical sunny days were that there was no rainfall or sudden changes in atmospheric temperature and humidity in the previous three days of the selected days. The mean and standard deviation of 24-h radon concentration in soil for the selected days are shown in Fig. 4, and the results except for 4.0 m depth of the three typical days were fitted with the 1D diffusion equation: $C_{Rn} = C_{\infty}(1 - e^{-\lambda Z})$ (Wang et al., 2021), where C_{∞} is the saturation concentration ($Bq \cdot m^{-3}$); λ is the effective diffusion coefficient (m^{-1}); and Z is the depth (m).

As shown in Fig. 4, soil radon concentration increased with depth, and the data from 0.1 to 3.0 m are generally consistent with the 1D diffusion equation. However, the radon concentration was unexpectedly low and extremely stable at 4.0 m throughout the three seasons, which might be attributed to a possible clay layer at this depth based on the observed soil color and texture. The precondition for the 1D diffusion equation is that the soil medium is homogeneous. Nevertheless, the special soil layer existing at 4.0 m does not satisfy this condition. Consequently, the value at 4.0 m is greatly deviated. The possible tight dense clay structure at 4.0 m makes the radon concentration lower and mostly constant with time. In addition, there is no remarkable difference in soil radon concentration at each depth between different seasons, except for those at 1.6 and 5.0 m. Compared with the two layers soil structure result of Antonopoulos-Domis (Antonopoulos-Domis et al., 2009), a more complex multi-layer structure of soil with temporal variation in radon concentration is suggested at this site (see section

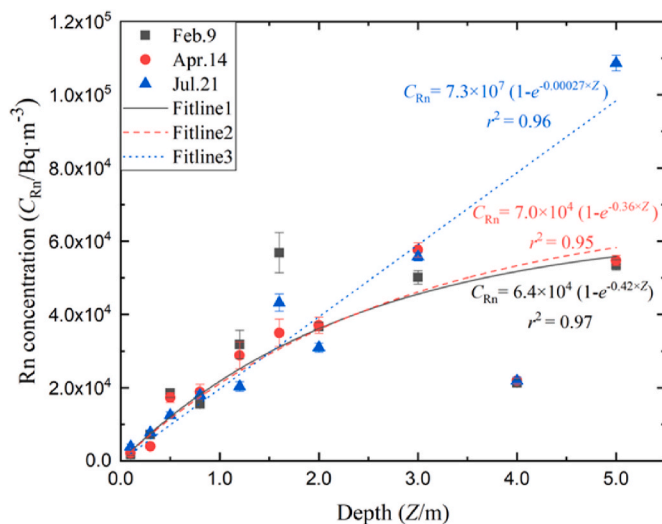


Fig. 4. Vertical distribution of one-day average soil radon concentrations in different seasons.

3.5). Furthermore, the larger sizes of error bars of soil radon concentration at 1.2 and 1.6 m depths (Fig. 4) indicate that radon concentration there has a dramatic variation in winter and spring. Further analysis in detail of their temporal variation is discussed below.

3.4. Temporal variation of radon concentration at different soil depths

To elucidate the temporal variation pattern of radon concentration in soil at different depths, the fast Fourier transform (FFT) was employed to analyze the two measurement periods of radon concentration time-series data. Considering the statistical errors in radiometric measurements, a 3-h moving average was employed before applying the FFT to minimize the irregular variations of radon concentration in soil. Fig. 5 shows the result of the FFT analysis within the period of 5–30 h for temporal variation at different depths.

As Fig. 5 shows, the soil radon concentrations at all ten depths in winter and spring (blue line) show larger periodic variations than those

in summer (orange line). It is presumed that the irregular and frequent rainfall in summer would disturb the diurnal variation pattern of radon concentration in the shallow soil, leading to the disappearance of large variations of radon concentration from 0.8 to 3.0 m depth in summer.

Diurnal variation of radon concentration at different soil depths can be obtained from the peak locations of FFT power. Similar to the variation of atmospheric radon concentration, the 24-h diurnal variation of soil radon concentration at 0.1 and 0.3 m depth in winter and spring might be affected by the temperature change of the shallow layer (Zhang et al., 2004). Soil radon concentration at 0.5–3.0 m depth shows a bi-periodic diurnal variation of 12 and 24 h (Fig. 5(b)). Especially at 1.2 and 1.6 m depth, the FFT power spectrums have sharper peaks, which

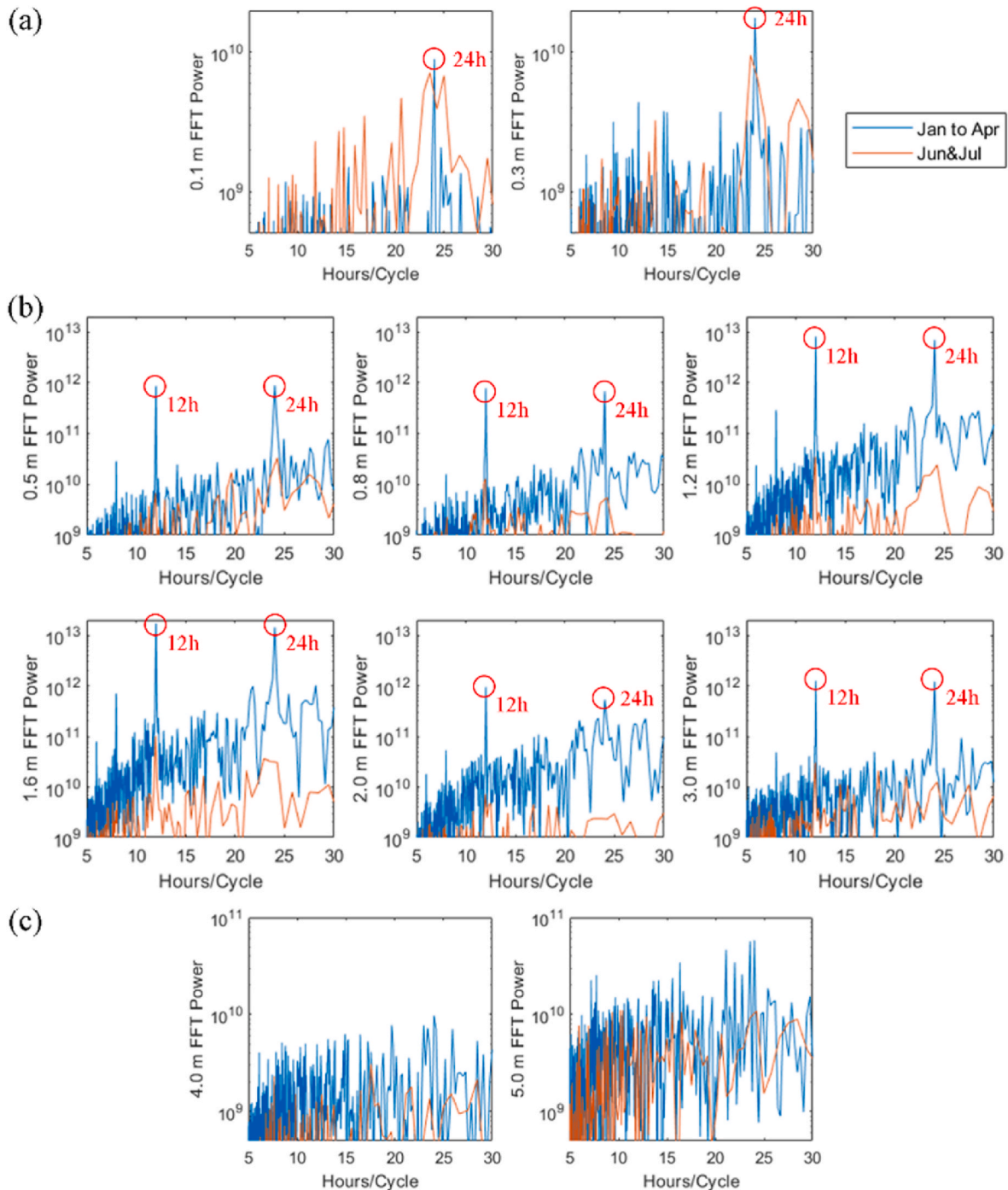


Fig. 5. FFT power-cycle spectrums of radon concentration in soil at ten different depths of two measurement periods: (a) 0.1 & 0.3 m; (b) from 0.5 to 3.0 m; and (c) 4.0 & 5.0 m.

indicate large 12-h and 24-h daily variation cycles. Soil radon concentrations at 4.0 and 5.0 m do not show diurnal variation regularity, which suggests that the meteorological parameters do not affect radon concentrations at this depth.

For further study on the correlation between the bi-periodic diurnal variation of soil radon concentration from 0.8 to 3.0 m depth and meteorological parameters in winter and spring, measurement results of one typical week with sunny and stable climate conditions in winter (February 6–13) and spring (April 13–20) were selected. The soil radon concentration data at 1.2 and 1.6 m in the same period were selected as representative. Results are shown in Fig. 6.

In Fig. 6, air temperature and humidity show obvious 24-h cyclical variations. Only air pressure shows a bi-periodic diurnal variation, which is quite similar to the diurnal variation pattern of soil radon concentration. To analyze the correlation between the diurnal variations of air pressure and the diurnal variations of radon concentration in soil, the influence of trends and variations with a more than 24-h cycle were excluded. The data of soil radon concentration and air pressure were smoothed by using a 24-h moving average. The original data were then deducted from the 24-h smoothed results to get the residual results. The residual results of soil radon concentration and air pressure are the diurnal variation components, as plotted in Fig. 7.

As Fig. 7 shows, soil radon concentration shows a bi-periodic diurnal variation, with the maximum value at 16:00, the second maximum value at 6:00, and the minimum values at 10:00 and 24:00. A bi-periodic diurnal variation of air pressure also existed. Nevertheless, the maximum and minimum values were just opposite to the extreme values of soil radon concentration, which suggests that the diurnal variations (residual results) of radon concentration at 1.2 and 1.6 m depth can be attributed to the variation of air pressure instead of the value of pressure itself. It indicated that there might be an exchange channel around this depth connected to the atmosphere, which might lead to a “breathing” process as reported by Miklyaev (Miklyaev et al., 2022).

3.5. Conceptualization of soil radon concentration at different depths

Based on the results of long-term observation and data analysis, a conceptualization of soil radon concentration and soil structure has been developed (Fig. 8).

At our study site, radon concentration in soil generally increased

with depth even at the quite deep depth of 3.0–5.0 m. The one exception was for 4.0 m depth where the distributions of water content, the radium concentration and the appearance of the soil (color and texture) suggested the existence of a clay layer. An air exchange channel might exist at 1.2–1.6 m, where the radon gas could be exchanged with the atmosphere easily, which leads to a large bi-periodic diurnal variation. The diurnal variation of soil radon concentration at 1.2 and 1.6 m depth has a negative correlation with the variation of air pressure, and radon concentration at nearby depths such as 0.8, 2.0 and 3.0 m also changes with time but with a smaller variation. This air exchange channel might disappear in summer, when rainfall changes the structure of the near-surface soil layer. At the depth of 5.0 m, there may be different complex soil structures when the level of the groundwater table changes in summer, which also might lead to a greater change of radon concentration in soil.

Overall, we consider that a complex layer structure of soil might exist at our study site and it might change with season. This study provides guidance for the study of radon behavior in soil and the change of soil structure by long-term online monitoring. It is useful for earthquake forecasting by employing detectors at different depths at the same time.

4. Conclusion

To systematically study the temporal variation of radon concentration in soil at different depths, a series of field measurements were carried out in a suburban area of Beijing. Soil radon concentration and meteorological parameters were continuously monitored for nearly three seasons. With the analysis of temporal variation in soil radon concentration and the comparison with meteorological parameters, the following conclusions are made:

1. In general, radon concentration increased with soil depth. However, a very stable and low radon concentration at 4.0 m was observed. The 1D diffusion model is not applicable to the radon concentration in soil at 4.0 m, where a possible clay layer exists and the radon concentration is not affected by meteorological parameters.
2. A bi-periodic diurnal variation of soil radon concentration was found at depths from 0.8 to 3.0 m, with the largest variation at 1.2 and 1.6 m in winter and spring. A negative correlation between the diurnal variation of soil radon concentration and the diurnal variation of air

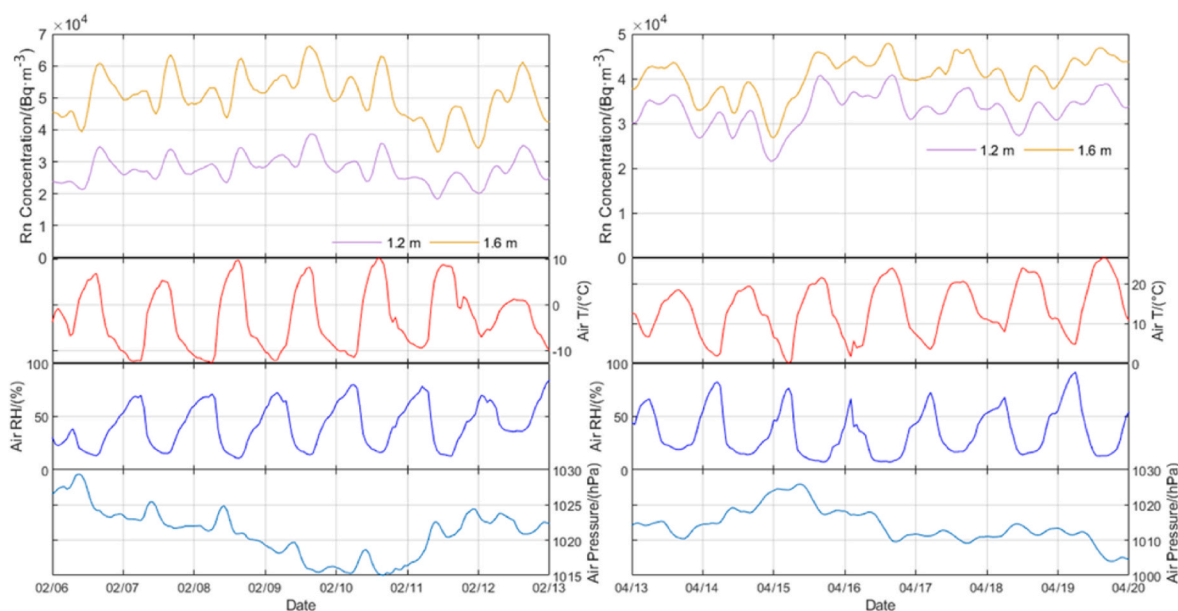


Fig. 6. One-week measurement results of radon concentration (after the moving average in 3 h) in soil at 1.2 and 1.6 m, air temperature, air relative humidity and air pressure in typical winter days (left, February 6–13) and spring days (right, April 13–20).

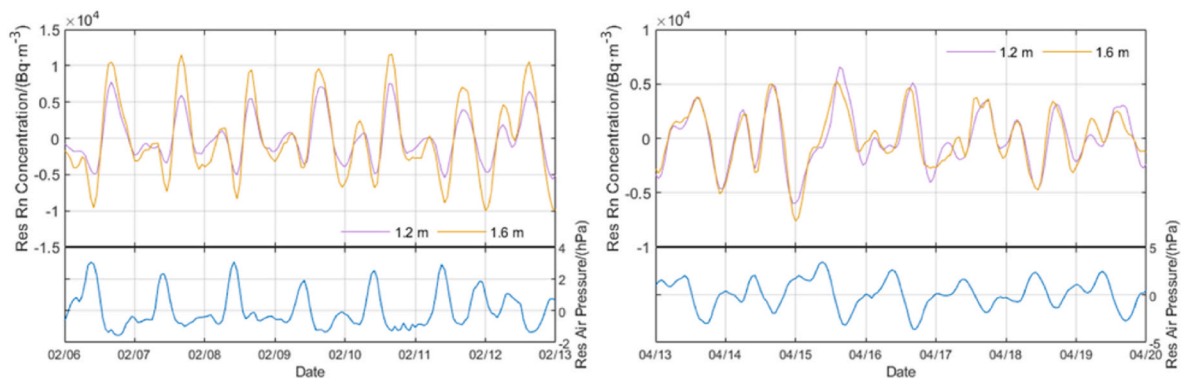


Fig. 7. 24-hour variation of residual results of soil radon concentration (upper part) and air pressure (lower part) (left: February 6–13; right: April 13–20).

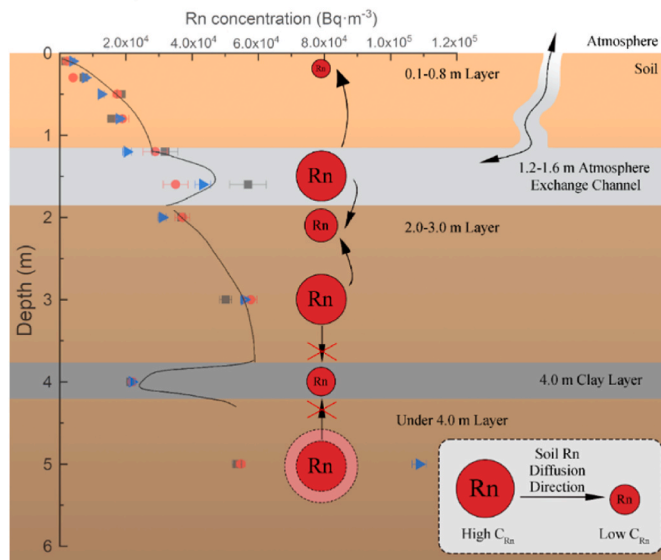


Fig. 8. Conceptualization of soil radon concentration and soil structure at the study site.

pressure was found. It is presumed that it comes from the exchange of soil radon with the atmosphere directly and it appears that the soil can “breathe”.

3. The radon concentration in soil was not affected by meteorological parameters at 5.0 m, but there was a long-range seasonal variation, which might be caused by seasonal fluctuations in groundwater level. The mechanism of radon concentration changes in deeper soil requires further study.
4. Irregular and frequent rainfall could disturb the diurnal variation of radon concentration in the near-surface soils, and the diurnal variation periodicity of radon concentration in summer was less clear than those in winter and spring.

The results of soil radon concentration in this case study indicate the complexity of soil structure. Each site or location may have a different soil structure. It is of great importance to understand the location's geological structure and complexity, which in practice could help make radon-in-soil a more effective tracer for geological applications. This study provides insights to the possible effects of soil structure on soil radon concentrations and may help in selecting appropriate depths for monitoring radon-in-soil for geological activities. Further studies should be carried out at more locations to obtain more typical regularities of radon-in-soil distribution.

Declaration of competing interest

The authors declare that they have no known competing financial interests or personal relationships that could have appeared to influence the work reported in this paper.

Data availability

Data will be made available on request.

Acknowledgement

We would like to thank the financial support of the State Key Laboratory of Nuclear Physics and Technology, School of Physics, Peking University and the National Natural Science Foundation of China (No.11975310, No.12275008).

Appendix A. Supplementary data

Supplementary data to this article can be found online at <https://doi.org/10.1016/j.jenvrad.2023.107200>.

References

- Antonopoulos-Domis, M., Xanthos, S., Clouvas, A., Alifrangis, D., 2009. Experimental and theoretical study of radon distribution in soil. *Health Phys.* 97 (4), 322–331.
- Barnet, Ivan, Pacherová, Petra, 2016. Gamma dose rate and soil gas radon concentration measured at low soil thickness (Czech Republic). *Environ. Earth Sci.* 75 (7), 1–7.
- Buttafuoco, G., Tallarico, A., Falcone, G., Guagliardi, I., 2010. A geostatistical approach for mapping and uncertainty assessment of geogenic radon gas in soil in an area of southern Italy. *Environ. Earth Sci.* 61 (3), 491–505.
- Catalano, R., Immé, G., Mangano, G., Morelli, D., et al., 2015. In situ and laboratory measurements for radon transport process study. *J. Radioanal. Nucl. Chem.* 306 (3), 673–684.
- Chen, Z., Li, Y., Liu, Z., et al., 2018. Radon emission from soil gases in the active fault zones in the Capital of China and its environmental effects. *Sci. Rep.* 8 (1), 1–12.
- Chen, Z., Li, Y., Liu, Z., Lu, C., Zhao, Y., Wang, J., 2019. Evidence of Multiple Sources of Soil Gas in the Tangshan Fault Zone. *Geofluids*, North China, 1945450.
- Cigolini, C., Gervino, G., Bonetti, R., Conte, F., Laiolo, M., Coppola, D., Manzoni, A., 2005. Tracking precursors and degassing by radon monitoring during major eruptions at Stromboli Volcano (Aeolian Islands, Italy). *Geophys. Res. Lett.* 32, 12.
- Das, N., Bhandari, R., Ghose, D., Sen, P., Sinha, B., 2009. Significant anomalies of helium, radon and gamma ahead of 7.9 M China earthquake. *Acta Geod. Geophys. Hung.* 44 (3), 357–365.
- Dhar, S., Randhawa, S.S., Kumar, A., Walia, V., Fu, C.C., Bharti, H., et al., 2021. Decomposition of continuous soil–gas radon time series data observed at Dharamshala region of NW Himalayas, India for seismic studies. *J. Radioanal. Nucl. Chem.* 327 (2), 1019–1035.
- Friedmann, H., 2012. Radon in earthquake prediction research. *Radiat. Protect. Dosim.* 149 (2), 177–184.
- Han, X., Li, Y., Du, J., Zhou, X., Xie, C., Zhang, W., 2014. Rn and CO₂ geochemistry of soil gas across the active fault zones in the capital area of China. *Nat. Hazards Earth Syst. Sci.* 14 (10), 2803–2815.
- Haquin, G., Zafrir, H., Ilzyer, D., Weisbrod, N., 2022. Effect of atmospheric temperature on underground radon: a laboratory experiment. *J. Environ. Radioact.* 253, 106992.
- Hwa, Oh, Yong, Kim, Guebuem, 2015. A radon-thoron isotope pair as a reliable earthquake precursor. *Sci. Rep.* 5 (1), 1–6.

- Kemski, J., Siehl, A., Stegemann, R., Valdivia-Manchego, M., 2001. Mapping the geogenic radon potential in Germany. *Sci. Total Environ.* 272 (1–3), 217–230.
- Measurement of Radioactivity in the Environment — Soil — Part 3: Test Method of Gamma-Emitting Radionuclides Using Gamma-Ray Spectrometry, 2015. ISO 18589-3.
- Miklyayev, Petr S., et al., 2022. Radon transport in permeable geological environments. *Sci. Total Environ.* 852, 158382.
- Mitev, K., Dutsov, C., Georgiev, S., Boshkova, T., Pressyanov, D., 2018. Unperturbed, high spatial resolution measurement of Radon-222 in soil-gas depth profile. *J. Environ. Radioact.* 196, 253–258.
- Nazaroff, William W., 1992. Radon transport from soil to air. *Rev. Geophys.* 30 (2), 137–160.
- Pinault, Jean-Louis, Baubron, Jean-Claude, 1996. Signal processing of soil gas radon, atmospheric pressure, moisture, and soil temperature data: a new approach for radon concentration modeling. *J. Geophys. Res. Solid Earth* 101 (B2), 3157–3171.
- Ren, H.W., Liu, Y.W., Yang, D.Y., 2012. A preliminary study of post-seismic effects of radon following the Ms 8.0 Wenchuan earthquake. *Radiat. Meas.* 47 (1), 82–88.
- Soil Quality — Determination of Dry Matter and Water Content on a Mass Basis — Gravimetric Method, 1993. ISO 11465.
- Sun, K., Guo, Q., Zhuo, W., 2004. Feasibility for mapping radon exhalation rate from soil in China. *J. Nucl. Sci. Technol.* 41 (1), 86–90.
- Vaupotič, J., Riggio, A., Santulin, M., Zmazek, B., Kobal, I., 2010. A radon anomaly in soil gas at Cazzaso, NE Italy, as a precursor of an ML= 5.1 earthquake. *Nukleonika* 55 (4), 507–511.
- Wang, H., Zhang, L., Wang, Y., Sun, C., Guo, Q., 2021. New-designed in-situ measurement system for radon concentration in soil air and its application in vertical profile observation. *J. Nucl. Sci. Technol.* 59 (2), 222–229.
- Yang, H.F., et al., 2021. Evolution of groundwater level in the North China Plain in the past 40 years and suggestions on its overexploitation treatment (in Chinese and with English abstract). *Chin. Geol.* 48 (4), 1142–1155.
- Zafirir, H., Ben Horin, Y., Malik, U., Chemo, C., Zalevsky, Z., 2016. Novel determination of radon-222 velocity in deep subsurface rocks and the feasibility to using radon as an earthquake precursor. *J. Geophys. Res. Solid Earth* 121 (9), 6346–6364.
- Zhang, L., Qiuju, G., Takao, I., 2004. Atmospheric radon levels in Beijing, China. *Radiat. Protect. Dosim.* 112 (3), 449–453.